Model Reduction for Linear and Nonlinear Gust Loads Analysis

A. Da Ronch*, N. D. Tantaroudas†, S. Timme‡ and K. J. Badcock§

University of Liverpool, Liverpool, England L69 3BX, United Kingdom

Time domain gust response analysis based on large-order nonlinear aeroelastic models is computationally expensive. An approach to the reduction of nonlinear models for gust loads prediction is presented in this paper. The method uses information on the eigenspectrum of the coupled system Jacobian matrix and projects the full order model through a series expansion onto a small basis of eigenvectors which is capable of representing the full order model dynamics. Linear and nonlinear reduced models derived from computational fluid dynamics and linear/nonlinear structural models are generated in this way. The novelty in the paper concerns the representation of the gust term in the reduced model in a manner consistent with standard synthetic gust definitions, allowing a systematic investigation of the influence of a large number of gusts without regenerating the reduced model. The methodology is illustrated by results for an aerofoil, with a combination of linear and nonlinear structural and aerodynamic models used, and a wing model with modal structural model.

Nomenclature

$\boldsymbol{A}$	= Jacobian matrix of $\boldsymbol{R}$ with respect to $\boldsymbol{w}$
$\boldsymbol{B}$, $\boldsymbol{C}$	= second and third Jacobian operators
b	= semichord
I_α	= second moment of inertia of aerofoil about elastic axis
m	= aerofoil sectional mass
S_α	= first moment of inertia of aerofoil about elastic axis
t	= physical time
x_α	= aerofoil static unbalance, $S_\alpha/m\,b$
$\boldsymbol{R}$	= residual vector
r_a	= radius of gyration of aerofoil about elastic axis, $r_a^2 = I_\alpha/m\,b^2$
U	= freestream velocity
U^*	= reduced velocity, $U/b\,\omega_\alpha$
$\boldsymbol{w}$	= vector of unknowns
$u_{g\,x}$, $u_{g\,y}$, $u_{g\,z}$	= gust vertical velocity
$u_{g\,0}$	= intensity of gust vertical velocity

Greek

α	= pitch angle
λ_i	= i-th eigenvalue of $\boldsymbol{A}$
τ	= nondimensional time, $t\,U/b$
ϑ	= scalar value scaling the generalised force term in the structural residual
ω_ξ	= uncoupled plunging mode natural frequency, $\sqrt{K_\xi/m}$

*Research Associate, School of Engineering; A.Da-Ronch@liverpool.ac.uk. Member AIAA (Corresponding Author).
†PhD Student, School of Engineering.
‡Lecturer, School of Engineering. Member AIAA.
§Professor, School of Engineering. Senior Member AIAA.

ω_α = uncoupled pitching mode natural frequency about elastic axis, $\sqrt{K_\alpha/I_\alpha}$
$\boldsymbol{\phi}_i$, $\boldsymbol{\psi}_i$ = i-th right and left eigenvectors of $\boldsymbol{A}$
$\bar{\omega}$ = ratio of ω_ξ/ω_α
ζ_ξ = damping ratio in plunge
ζ_α = damping ratio in pitch
Ξ = structural mode shape matrix
ξ = nondimensional displacement in plunge, h/b
μ = mass ratio, $m/\pi\,\rho\,b^2$
ρ = freestream density

Symbol

$\dot{(\,)}$ = differentiation with respect to t, $d(\,)/dt$
$(\,)'$ = differentiation with respect to τ, $d(\,)/d\tau$
$\bar{(\,)}$ = complex conjugation

I. Introduction

In flight, aircraft regularly encounter atmospheric turbulence. The turbulence is regarded for linear analysis as a set of component velocities (gusts) superimposed on the background steady flow. The aircraft experiences rapid changes in lift and moment forces, which cause rigid and flexible dynamic responses of the entire aircraft. These responses can cause passenger discomfort and introduce large loads on the structure which must be accounted for during the design stage to ensure aircraft safety. The loads encountered at high angles of attack form some of the critical cases used in the structural sizing of the aircraft components for a passenger jet. The capability to calculate these loads with a high degree of accuracy would allow reduced conservatism without compromising safety. Currently conservatism is necessary because of the limited certainty of the possible forms of atmospheric gusts and the limited realism for some flow regimes of linear methods currently used to predict the aircraft response.

The well-established methods for gust loads calculations are based on linear aerodynamic models which are solved in the frequency domain. More recently, for very flexible aircraft, the gust analysis has seen the use of low- to medium-fidelity aerodynamic models. Two-dimensional potential theory and panel methods were the common choice.[1,2] Limiting assumptions in the aerodynamics restrict the validity of simulations to linear flow conditions, e.g. low angles of attack and low speed. The use of high-fidelity models based on computational fluid dynamics (CFD) has been reported, for example, in Ref.[3] Grid velocities are used to apply a disturbance in a time domain CFD calculation,[4] overcoming the problems associated with numerical dissipation of the disturbance but also removing the influence of the aircraft flow field and motion on the gust.

The cost of time domain calculations makes the routine use of CFD in gust response analysis unrealistic, and system-identification methods have been used as a cheaper alternative. Proper Orthogonal Decomposition has been used as a model reduction technique to generate reduced models for gust simulations, but suffers from the usual limitations related to the necessity for a set of training data closely related to the final application cases, and the difficulty of accounting for nonlinearity in the reduced model. A systematic and cost effective approach to developing reduced models capable of describing both linear and nonlinear effects for a range of cases based on limited development cost has, to date, proved elusive.

An approach to calculating a reduced order model from a large dimension CFD model which can calculate a nonlinear response has been reviewed in Ref.[5] The method first calculates the important modes of the problem from a large order eigenvalue problem. For an aeroelastic limit-cycle oscillation (LCO), the system responds in the critical mode close to the bifurcation point. The approach presented in Refs.[6,7] is to project the full-order model onto the critical mode and expand the residual in a Taylor series, retaining quadratic and cubic terms. The influence of the noncritical space on the critical mode is included through a centre manifold approximation. The method has been successfully applied to various test cases, including the LCO prediction dominated by the motion of a shock wave[6] and a prototype flight dynamics instability of a delta wing.[7] The approach to model reduction has been generalized in Ref.[8] by using multiple coupled system eigenmodes for model projection and introducing control deflection and gust interaction effects in the formulation. The method has several strengths, namely (i) that it exploits information from the stability

(flutter) calculation for the development of a ROM for dynamic response analyses; (ii) linear or nonlinear reduced models can be developed within the same framework; (iii) the reduced model can be parametrised to avoid ROM regeneration.

The current paper tackles the problem of how to introduce gust terms into the reduced model to allow a gust loads analysis to be carried out. The paper continues with the formulation of the full and reduced models. Then a new approach to calculating the gust term is proposed. Results are then given for an aerofoil and wing problem to evaluate the method from the point of view of accuracy and computational efficiency. Finally conclusions are drawn. The important features of the method developed are (i) linear and nonlinear ROMs can be developed; (ii) the model reduction is performed once, with application of any gust made without further recourse to the CFD code.

II. Full and Reduced Order Models

II.A. Full Order Model

The full order nonlinear aeroelastic model is written in state-space form. Denote by $\boldsymbol{w}$ the n-dimensional state-space vector which is conveniently partitioned into fluid and structural degrees of freedom

$$\boldsymbol{w} = \left[\boldsymbol{w}_f^T, \boldsymbol{w}_s^T\right]^T \tag{1}$$

In the case that CFD is used as the source of the aerodynamic predictions, the vector $\boldsymbol{w}_f$ may contain millions of unknowns. The state-space equations in the general vector form are

$$\frac{\mathrm{d}\boldsymbol{w}}{\mathrm{d}t} = \boldsymbol{R}(\boldsymbol{w}, \boldsymbol{u}_d) \tag{2}$$

where $\boldsymbol{R} = \left[\boldsymbol{R}_f^T, \boldsymbol{R}_s^T\right]^T$ is the (nonlinear) residual and $\boldsymbol{u}_d$ is a vector denoting an externally applied disturbance acting on the system. The homogeneous system has an equilibrium solution, $\boldsymbol{w}_0$, for given constant $\boldsymbol{u}_{d\,0}$ corresponding to a constant solution in the state space and satisfying

$$\frac{\mathrm{d}\boldsymbol{w}_0}{\mathrm{d}t} = \boldsymbol{R}(\boldsymbol{w}_0, \boldsymbol{u}_{d\,0}) = \boldsymbol{0} \tag{3}$$

The system often also includes an independent parameter (freestream speed, air density, altitude, etc.) which is varied to study stability of the equilibria.

The residual function in Eq. (2) forms the basis for the model reduction method described below. The options for the residual evaluation are described in the next section.

II.B. Residual Definition

The formulation of the previous section is given in terms of the residual function $\boldsymbol{R}$. Several options are used in this paper to define the residual, giving modelling at different levels of fidelity and computational cost. The options are summarised in this section.

II.B.1. Computational Fluid Dynamics

The first CFD code used is the Parallel Meshless solver of the University of Liverpool which solves the Euler, laminar and Reynolds-Averaged Navier-Stokes equations (with the Spalart-Almaras turbulence model) on a point cloud. This code is used to compute the aerofoil results shown below. The solver is summarised in Ref.[9] The unknowns are stored at each (star) point, and a cloud of surrounding points is defined for the spatial discretisation. The definition of this stencil is a non-trivial problem which is solved using the method described in Ref.,[10] which exploits information from point connectivity in underlying component meshes to guide the search ellipses for the stencil. Successive application of this method allows the stencils to be updated for moving geometries, providing great flexibility for the problems that can be computed.

Osher's approximate Riemann solver is used to evaluate the convective fluxes at the mid point between the star point and every other point in the stencil. A least squares reconstruction is calculated at each star point to estimate the gradients of the flow unknowns there also. These gradients are then used to provide a high order reconstruction of the interface values for the Riemann problem, with the reconstruction limited to

avoid oscillations by the Barth and Jespersen limiter. A least squares reconstruction of the mid point fluxes is then used to calculate the gradients required for the residual. The star point gradients are used to calculate the terms needed for the viscous fluxes, which are averaged to the mid-points and then reconstructed as for the convective fluxes to obtain the required viscous contributions to the residual. At each stage it is straightforward to use the chain rule to calculate the Jacobian matrix contributions analytically. The steady state CFD solver uses an implicit method which drives convergence using the Jacobian matrix, solving a linear system for the updates with a preconditioned Krylov sparse matrix solver. For moving body problems a number of options for moving the point clouds are available, but in the current paper there is only the requirement to move points rigidly with aerofoil. Time accurate calculations are done using the pseudo time stepping method, which solves a modified steady state problem for the updated solution at each new time step. The treatment of gusts is described in the section below.

The second CFD code used in this paper, which is applied to the three dimensional case computed, is based on the University of Liverpool parallel multiblock solver. The Euler equations are discretized on curvilinear multiblock body-conforming grids using a cell-centered finite-volume method. The residual is formed using Osher's approximate Riemann solver with the monotone upwind scheme for conservation laws interpolation. Exact Jacobian matrices are formed. The mesh can be deformed using transfinite interpolation. The steady state and time accurate solvers are identical to those used for the meshless code described above. More details on the CFD formulation can be found in Ref.,[11] and on the application to problems in aeroelasticity in Ref.[5]

II.B.2. Linear Aerodynamic Model

A computationally cheaper alterative to the CFD model is based on strip theory and the incompressible two–dimensional classical theory of Theodorsen. The total aerodynamic loads consist of contributions arising from the section motion, flap deflection and the penetration into a gusty field. The aerodynamic loads due to an arbitrary input time-history are obtained through convolution against a kernel function. For the influence of the aerofoil motion on the loads, the Wagner function is used. For the response to a sharp edged gust, the integration uses the Küssner function. Since the assumption is of linear aerodynamics, the effects of the two influences on the aerodynamic forces and moments are added together to find the variation of the forces and moments in time for a given motion and gust. For a practical evaluation of the integral, an exponential approximation is used for the Wagner and Küssner functions. The aerodynamic state vector for this model has dimension 8, and the formulation in terms of a residual function follows that given in Ref.[12]

II.B.3. Two Degree-of-Freedom Model

The aerofoil shown in Fig. 1 has two degrees of freedom that define the motion about a reference elastic axis (*e.a.*). The plunge deflection is denoted by h, positive downward, and α is the angle of attack about the elastic axis, positive with nose up. The aerofoil is equipped with a massless trailing-edge flap with hinge at a distance $c\,b$ from the midchord. The flap deflection, δ, is defined relative to the undeflected position. The motion is restrained by two springs, K_ξ and K_α, and is assumed to have a horizontal equilibrium position at $h = \alpha = \delta = 0$. The system also contains structural damping in both degrees of freedom.

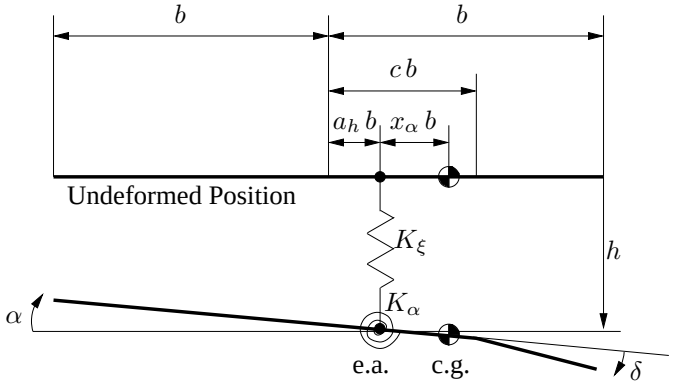

Figure 1. Schematic of an aerofoil section with trailing-edge flap; the wind velocity is to the right and horizontal; e.a. and c.g. denote, respectively, the elastic axis and centre of gravity (from Ref.[8])

The equations of motion in dimensional form with nonlinear restoring forces in pitch and plunge can be derived, for example, using the Lagrange equations[13]

$$m\,\ddot{h} + S_\alpha\,\ddot{\alpha} + C_\xi\,\dot{h} + K_\xi\left(h + \beta_\xi\,h^3 + \beta_{\xi_5}\,h^5\right) = -L \tag{4}$$

$$S_\alpha\,\ddot{h} + I_\alpha\,\ddot{\alpha} + C_\alpha\,\dot{\alpha} + K_\alpha\left(\alpha + \beta_\alpha\,\alpha^3 + \beta_{\alpha_5}\,\alpha^5\right) = M \tag{5}$$

with the structural nonlinearity approximated in a polynomial form.[14] The lift, L, is defined positive upward according to the usual sign convention in aerodynamics. The plunge displacement, h, is positive downward, as it is conventionally done in aeroelasticity. In nondimensional form, the equations of motion become

$$\xi'' + x_\alpha\,\alpha'' + 2\,\zeta_\xi\,\frac{\bar{\omega}}{U^*}\,\xi' + \left(\frac{\bar{\omega}}{U^*}\right)^2\left(\xi + \beta_\xi\,\xi^3 + \beta_{\xi_5}\,\xi^5\right) = -\frac{1}{\pi\,\mu}\,C_L\,(\tau) \tag{6}$$

$$\frac{x_\alpha}{r_a^2}\,\xi'' + \alpha'' + 2\,\zeta_\alpha\,\frac{1}{U^*}\,\alpha' + \left(\frac{1}{U^*}\right)^2\left(\alpha + \beta_\alpha\,\alpha^3 + \beta_{\alpha_5}\,\alpha^5\right) = \frac{2}{\pi\,\mu\,r_a^2}\,C_m\,(\tau) \tag{7}$$

where nondimensional parameters are defined in the nomenclature. Differentiation with respect to t, indicated by $\dot{(\,)}$, is replaced by a differentiation with respect to τ, $\dot{(\,)} = U/b\,(\,)'$. These equations are rewritten to define a residual contribution.

II.C. Modal Structural Model

As given in Ref.,[5] for general linear structural motions, the dimensionless structural equations of motion are defined in physical coordinates as

$$\boldsymbol{M}\delta\ddot{\mathbf{x}}_s + \boldsymbol{C}\delta\dot{\mathbf{x}}_s + \boldsymbol{K}\delta\mathbf{x}_s = \vartheta\,\mathbf{f}. \tag{8}$$

The deflections $\delta\mathbf{x_s}$ of the (linear) structure are defined at the set of physical coordinates $\mathbf{x}_s$ by $\delta\mathbf{x}_s = \Xi\,\boldsymbol{\eta}$, where the vector $\boldsymbol{\eta}$ contains the generalised coordinates (modal amplitudes). The columns of the matrix Ξ contain the mode shape vectors evaluated from a finite–element model of the structure with the deflections defined at the structural grid points. Projecting the finite–element equations onto the mode shapes, while scaling to obtain generalised masses of magnitude one (i.e. $\Xi^T\boldsymbol{M}\Xi = \boldsymbol{I}$ with $\boldsymbol{I}$ as the identity matrix) gives a system of scalar equations written in state–space with the structural residual given by

$$\mathbf{R}_s = \begin{bmatrix} \mathbf{0} & \boldsymbol{I} \\ -\Xi^T\boldsymbol{K}\Xi & -\Xi^T\boldsymbol{C}\Xi \end{bmatrix}\mathbf{w}_s + \begin{bmatrix} \mathbf{0} \\ \boldsymbol{I} \end{bmatrix}\vartheta\,\Xi^T\mathbf{f} \tag{9}$$

and the vector of structural unknowns $\mathbf{w}_s = [\boldsymbol{\eta}^T, \dot{\boldsymbol{\eta}}^T]^T$ containing the generalised coordinates and their velocities. The vector $\mathbf{f}$ of aerodynamic (pressure) forces at the structural grid points follows from the wall pressure, the area of the surface segment and the unit normal vector, and thus is a function of fluid and structural unknowns. It is then projected using the mode shapes to obtain the generalised forces $\Xi^T\mathbf{f}$. The parameter ϑ for the mass ratio is obtained from the nondimensionalisation of the governing equations and depends on the reference density and the reference length. The method used to transfer the surface pressure forces to the structural nodes is described in Ref.[5]

II.D. Model Reduction

Denote by $\Delta\boldsymbol{w} = \boldsymbol{w} - \boldsymbol{w}_0$ the increment in the state-space vector with respect to an equilibrium solution. The large-order nonlinear residual formulated in Eq. (2) is expanded in a Taylor series around the equilibrium point

$$\boldsymbol{R}\,(\boldsymbol{w}) \approx \boldsymbol{A}\,\Delta\boldsymbol{w} + \frac{\partial\,\boldsymbol{R}}{\partial\,\boldsymbol{u}_d}\,\Delta\boldsymbol{u}_d + \frac{1}{2}\,\boldsymbol{B}\,(\Delta\boldsymbol{w},\,\Delta\boldsymbol{w}) + \frac{1}{6}\,\boldsymbol{C}\,(\Delta\boldsymbol{w},\,\Delta\boldsymbol{w},\,\Delta\boldsymbol{w}) + \mathcal{O}\left(|\Delta\boldsymbol{w}|^4\right) \tag{10}$$

retaining terms up to third order in the perturbation variable. The Jacobian matrix of the system is denoted as $\boldsymbol{A}$ and the vectors $\boldsymbol{B}$ and $\boldsymbol{C}$ indicate, respectively, the second and third order Jacobian operators. The full-order system is projected onto a basis formed by a small number (denoted by m) of eigenvectors of the Jacobian matrix evaluated at the equilibrium position. Right and left eigenvectors are scaled to satisfy

the biorthonormality conditions.[8] The projection of the full-order model is done using a transformation of coordinates

$$\Delta \boldsymbol{w} \;=\; \boldsymbol{\Phi}\,\boldsymbol{z} \;+\; \bar{\boldsymbol{\Phi}}\,\bar{\boldsymbol{z}} \tag{11}$$

where $\boldsymbol{z} \in \mathbb{C}^m$ is the state-space vector governing the dynamics of the reduced-order nonlinear system and $\boldsymbol{\Phi}$ is the modal matrix of right eigenvectors. The result is a system of ordinary differential equations in $\boldsymbol{z}$ which have linear, quadratic and cubic terms in $\boldsymbol{z}$ and $\bar{\boldsymbol{z}}$. The coefficients of these terms are derived by using matrix free approximations for the first, second and third order Jacobians applied to combinations of the columns of $\boldsymbol{\Phi}$ (i.e. the basis vectors for the reduction). The matrix free approximations work on residual evaluations, but require extended order arithmetic to be used to obtain accurate approximations. The full details of the methodology are given in Refs.[6,8,15]

A major computational challenge arises when using CFD as the source of the aerodynamic predictions. The solution of a large sparse linear system arising from an eigenvalue problem is needed for model generation, see Eq. (11). To overcome this, the Schur complement eigenvalue formulation is used. The method leads to a small nonlinear eigenvalue problem that can be solved rapidly by removing the need to solve large sparse linear systems that are almost singular. The coupled system Jacobian matrix of Eq. (2) is most conveniently done by partitioning the matrix as

$$\boldsymbol{A} \;=\; \begin{bmatrix} \frac{\partial \boldsymbol{R}_f}{\partial \boldsymbol{w}_f} & \frac{\partial \boldsymbol{R}_f}{\partial \boldsymbol{w}_s} \\ \frac{\partial \boldsymbol{R}_s}{\partial \boldsymbol{w}_f} & \frac{\partial \boldsymbol{R}_s}{\partial \boldsymbol{w}_s} \end{bmatrix} \;=\; \begin{bmatrix} \boldsymbol{A}_{ff} & \boldsymbol{A}_{fs} \\ \boldsymbol{A}_{sf} & \boldsymbol{A}_{ss} \end{bmatrix} \tag{12}$$

The block $\boldsymbol{A}_{ff}$ represents the influence of the fluid unknowns on the fluid residual and has by far the largest number of non-zeros for the structural models used. The term $\boldsymbol{A}_{fs}$ arises from the dependence of the CFD residual on the mesh motion and speeds, which depend in turn on the structural solution, and is evaluated by finite difference. The term $\boldsymbol{A}_{sf}$ is due to the dependence of the generalized forces on the surface pressures. Finally, the block $\boldsymbol{A}_{ss}$ is the Jacobian of the structural equations with respect to the structural unknowns.

Write the coupled system eigenvalue problem as

$$\begin{bmatrix} \boldsymbol{A}_{ff} & \boldsymbol{A}_{fs} \\ \boldsymbol{A}_{sf} & \boldsymbol{A}_{ss} \end{bmatrix} \boldsymbol{p} \;=\; \lambda\,\boldsymbol{p} \tag{13}$$

where $\boldsymbol{p}$ and λ are the complex eigenvector and eigenvalue, respectively. Partition the eigenvector as

$$\boldsymbol{p} \;=\; \left[\boldsymbol{p}_f^T,\, \boldsymbol{p}_s^T\right]^T \tag{14}$$

By substituting $\boldsymbol{p}_f$ from the first set of equations into the second set of equations in Eq. (13), it can be found that the eigenvalue λ, assuming it is not an eigenvalue of $\boldsymbol{A}_{ff}$, satisfies the nonlinear eigenvalue problem

$$\boldsymbol{S}\,(\lambda)\;\boldsymbol{p}_s \;=\; \lambda\,\boldsymbol{p}_s \tag{15}$$

where $\boldsymbol{S}\,(\lambda) = \boldsymbol{A}_{ss} - \boldsymbol{A}_{sf}\,(\boldsymbol{A}_{ff} - \lambda I)^{-1}\,\boldsymbol{A}_{fs}$. The matrix $\boldsymbol{S}\,(\lambda)$ is the sum of the structural matrix and a second term arising from the coupling of the fluid and structure. The nonlinear Eq. (15) is solved using Newton's method. To overcome the cost of forming the residual and its Jacobian matrix at each iteration, an approximation of $(\boldsymbol{A}_{ff} - \lambda I)^{-1}$ is used. More details on the Schur complement eigenvalue solver and its application to realistically sized aeroelastic models can be found in Ref.[16]

III. Gust Treatment

III.A. Overview

The determination of the worst case structural forces from an encounter with idealised atmospheric disturbances is an important problem in aircraft design.[17] The atmospheric disturbances are characterised either as discrete gusts or as continuous disturbances defined by a frequency power spectrum and the Gaussian distribution for the frequency content at any particular time. In either case the disturbance is specified as a change in the freestream airflow over the aircraft. Established analysis methods are linear, using potential flow aerodynamics. This allows superposition and frequency domain calculations to be exploited. In the

current paper, linear predictions of the forces and moments for an aerofoil interacting with a gust are computed by adding contributions from convolution integrals to account for the influence of the aerofoil motion and the gust interaction. In CFD simulations the specification of the gust is more complicated. First, the frequency domain formulation is nonlinear, meaning that the calculation is likely to be done in the time domain, implying a high computational cost and that each gust must be analysed with a new calculation. Secondly, in principal it is straightforward to apply an atmospheric disturbance as a far field boundary condition. In practice however, numerical dissipation makes it difficult to propagate this disturbance to the interaction with the aircraft. To overcome this problem a simpler simulation is formulated that applies the disturbance to the mesh velocities only. This does not allow for the gust to be modified by the interaction. In the following section the model reduction method is used to address the first problem.

III.B. Treatment in Computational Fluid Dynamics Model

The approach in Ref.,[4] referred to as the field-velocity approach, has been used for gust calculations[18] and is also exploited in this work. The gust is introduced into the CFD solver by modification of the velocity of grid points during the unsteady motion of the aircraft. A disadvantage of the field-velocity approach is that the gust is assumed frozen, and the influence of the structural response on the gust is neglected. The approach has received widespread use because of the lack of alternative methods.

Denote the disturbance vector by

$$\Delta \boldsymbol{u}_d \;=\; [u_{g\,x},\, u_{g\,y},\, u_{g\,z}]^T \tag{16}$$

This time dependent vector is applied to the mesh velocities before the calculation of the residual. Without loss of generality, the model reduction is illustrated for the vertical component of gust velocity, $u_{g\,z}$.

The new challenge is to calculate a term in the reduced model to represent the gust. The term required corresponds to the term in Eq. (10) given by

$$\frac{\partial\, \boldsymbol{R}}{\partial \boldsymbol{u}_d}\, \Delta \boldsymbol{u}_d.$$

The derivation of the term should be independent of the gust allowing different gusts to be applied to the reduced model without any recalculation.

Using the chain rule, the dependence of the nonlinear full-order residual on the gust perturbation is rewritten as

$$\frac{\partial \boldsymbol{R}}{\partial u_{g\,z}} \;=\; \frac{\partial \boldsymbol{R}}{\partial \dot{\boldsymbol{z}}}\, \frac{\partial \dot{\boldsymbol{z}}}{\partial u_{g\,z}} \tag{17}$$

where $\dot{\boldsymbol{z}}$ is the mesh velocity vector. The first term on the right side depends on point coordinates only and can be computed independent of the gust definition using finite differences or analytical differentiation.

The second term on the right side of Eq. (17) depends on both spatial and temporal coordinates because the prescribed gust is generally a function of space and time, $u_{g\,z}\,(x, y, z, t)$. The gust simulation using a ROM, as formulated in Ref.,[8] requires the calculation at each time step of the contribution arising from

$$\bar{\boldsymbol{\psi}}_i^T\, \frac{\partial \boldsymbol{R}}{\partial \dot{\boldsymbol{z}}}\, \frac{\partial \dot{\boldsymbol{z}}}{\partial u_{g\,z}} \tag{18}$$

where $\bar{\boldsymbol{\psi}}$ is the matrix of eigenvectors of $\boldsymbol{A}^T$. The first two terms on the left side involve a matrix-vector multiplication, and this can be done before the time-domain ROM simulation. At each time step iteration, the vector on the right side needs to be updated to account for the gust translation, and the scalar product of two vectors is then needed. Therefore, at each time step of the ROM, an inner product of two vectors of the dimension of the CFD mesh is needed, increasing the cost of calculating solutions by the ROM. However, the CFD code does not need to be accessed for this operation, which requires only the grid point coordinates, and the ROM can be applied to any definition of discrete or continuous gust. Results to illustrate the computational cost are given below.

IV. Aerofoil Results

IV.A. Test Case

The test problem considered is for the NACA 0012 aerofoil at zero incidence. The parameters for the structural model are given in Table 1. The test case corresponds to the "heavy case" described in Ref.[19] The point distribution near the aerofoil used for the Euler calculations is shown in Fig. 2 and consists of 7974 grid points.

Parameter	Value
$\bar{\omega}$	0.343
μ	100.0
a_h	-0.2
x_α	0.2
r_α	0.539

Table 1. Reference values of the pitch-plunge aerofoil model

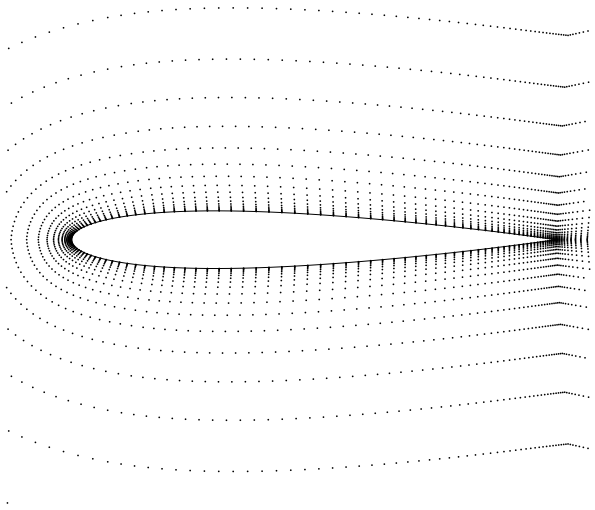

Figure 2. Point distribution for NACA 0012 aerofoil

Starting with an evaluation of the steady state CFD prediction at a Mach number of 0.85 and an angle of attack of 1.0 deg, a comparison is made in Fig. 3 for results on 7974 points, a medium point cloud of 22380, a finer point cloud of 88792 points, and measurements from Ref.[20] The agreement for the solution on the point cloud used for the gust calculations below is satisfactory.

IV.B. Flutter Analysis

The model reduction requires the coupled system (i.e. aeroelastic) eigenvectors as input. These are obtained from an eigenvalue analysis that also provides the flutter speed. This was done for the CFD aerodynamics model using the Schur method summarised above. More specifically, the expensive term in the calculation, $(A_{ff} - \lambda I)^{-1}$, is expanded in a first order Taylor series about a chosen shift λ_0, which is based on the structural frequencies, and then the eigenvalue problem in Eq. (15) for increasing values of the reduced velocity is solved easily for the deviation from this shift. The expansion requires pre–computations with the right–hand side A_{fs}. Linear systems are solved using a preconditioned generalized conjugate residual sparse iterative solver. Preconditioning with complex arithmetic uses an incomplete lower upper factorisation of an approximation to the coefficient matrix $(A_{ff} - \lambda_0 I)$ where the approximation is based on a combination of first and second order spatial discretisations for A_{ff} as described in Ref. [21] One level of fill–in during the factorisation is allowed and sufficient.

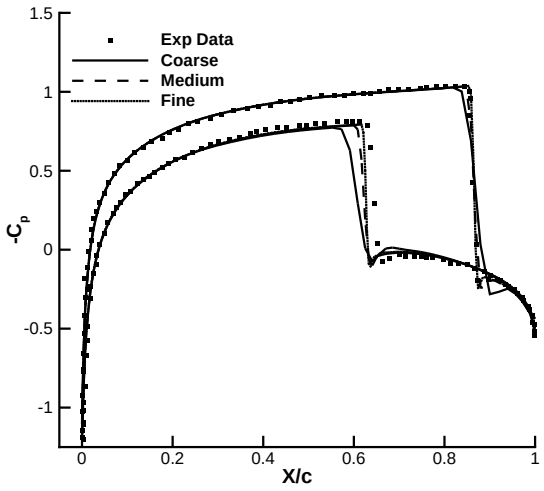

Figure 3. Comparison of the pressure distribution for NACA 0012 aerofoil at $M_\infty = 0.85$ and $\alpha = 1.0$ deg for three point cloud densities and the measurements of Ref.[20]

The traces of the aeroelastic eigenvalues with reduced velocity for a fixed Mach number of 0.8 are shown in Fig. 4 and show that the flutter speed in terms of the reduced velocity is about 3.577. The eigenvectors for the model reduction at this Mach number were computed for a reduced velocity of 2.0, as a representative condition in this paper. Tests at various reduced velocities confirmed in all cases the assessment of the reduced model made here for $U^* = 2.0$.

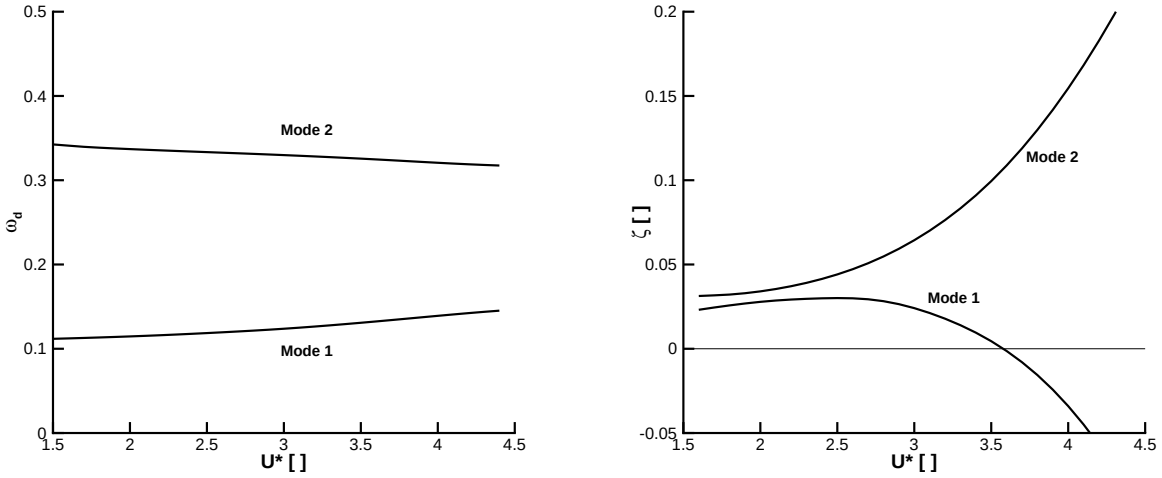

(a) Damped natural frequency, ω_d

(b) Damping ratio, ζ

Figure 4. Trace of the aeroelastic eigenvalues using CFD as a function of reduced velocity for a Mach number of 0.8

IV.C. Evaluation of the Reduced Model

The reduced model was calculated for the linear aerodynamic and CFD models, and the structural nonlinearity. Two aeroelastic modes associated with the pitching and plunging motions were retained. An evaluation of introducing additional modeshapes in the reduced model was presented in Ref.[8] and is not repeated here. There are several options for the number of terms retained in the reduced model. In the current work, the linear dynamic models have been used as they proved adequate to represent the gust response. This was

tested by comparison with the full order model, which is nonlinear. If this had not been the case then the option was there to include quadratic and cubic terms in a straightforward fashion. The form of the reduced model at a freestream Mach number of 0.8 without the gust term is

$$\frac{\mathrm{d}\boldsymbol{z}}{\mathrm{d}t} = \begin{bmatrix} \lambda_1 & 0 \\ 0 & \lambda_2 \end{bmatrix} \boldsymbol{z} \tag{19}$$

where $\lambda_1 = -1.00031 \cdot 10^{-2} + i \cdot 3.60176 \cdot 10^{-1}$ and $\lambda_2 = -3.61915 \cdot 10^{-2} + i \cdot 1.05872$.

The reduced models were first tested for a problem without a gust, involving the free response to an initial perturbation, $\xi' = 0.01$. The time response from the reduced and full order methods is shown in Fig. 5, and show that the CFD and linear results are close at the lower Mach number, and significantly different at the transonic Mach number, as expected. More importantly, in all cases the corresponding full order and reduced order model predictions were indistinguishable.

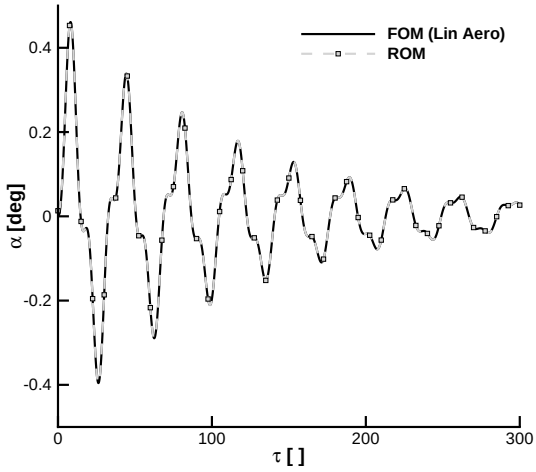

(a) Pitch, incompressible flow

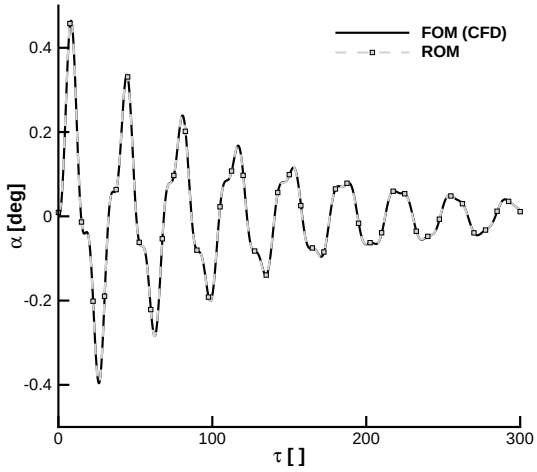

(b) Pitch at $M = 0.3$

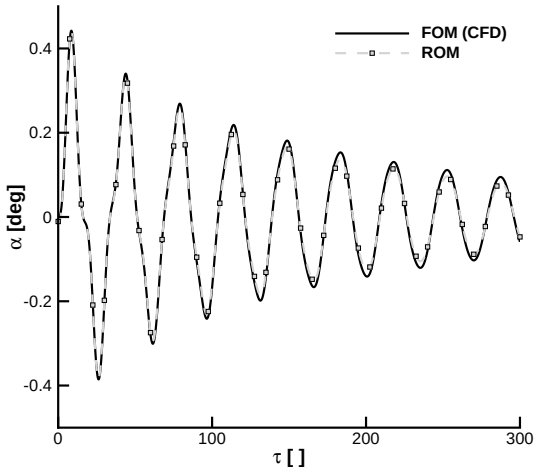

(c) Pitch at $M = 0.8$

Figure 5. Free response comparisons using CFD and linear aerodynamics at $\mathbf{U}^* = 2.0$ for two Mach numbers and initial condition $\xi' = 0.01$

Next, the gust term was added to the reduced model, and the reduced predictions were compared with

a full order calculation of the same case. The gust used was the "1 minus cosine" gust with an intensity of 1% of the freestream speed and a length of 25 semi-chords. The comparison for the case with a freestream Mach number of 0.8 is shown in Fig. 6 and again shows a good agreement between the reduced and full model results. However, some discrepancies between the models are observed for small times. While the peak to peak amplitude between two consecutive peaks predicted by the reduced model is in agreement with the full model results, the actual values at the first peak differ somewhat. A reason for this could be that the reduced model is initially driven by a perturbation which does not belong to the eigenvector basis used in the model projection, Eq. (11), or that some information on the gust term is missing. More modes could be added to enhance the eigenvector basis, as shown in Ref.[8]

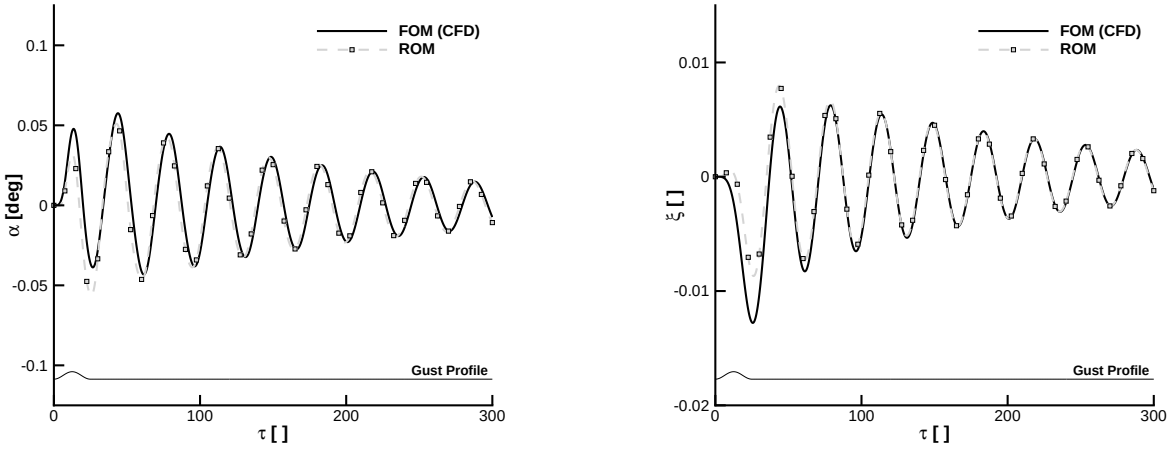

(a) Pitch, α

(b) Plunge, ξ

Figure 6. Response to a "1 minus cosine" gust with intensity of 1% of the freestream speed and a gust length of 25 at Mach 0.8.

The cost of the models is shown in Table 2. The time domain response was computed with nondimensional time step of 0.05 for 2000 iterations. Note that the cost of ROM generation is incurred once, and includes the costs of forming the eigenvector basis and of calculating the gust term. The gust coefficient matrix was computed in a brute force fashion by finite differences with two residual evaluations for each cloud point in the absence of an analytic evaluation, which would reduce drastically the time required for this step. The time domain response of the reduced model for any type of gust disturbance, e.g. discrete and continuous, is about 2 orders of magnitude faster than the full order calculation.

Item	Cost (sec)
Time Domain Full Order Calculation	5105
Reduced Model Generation	444
a) Calculating Eigenvector Basis	148
b) Calculating Gust Influence Matrix	296
Time Domain Reduced Model Calculation	68

Table 2. Computational cost summary

IV.D. Worst Case Gust Response for Discrete Gust

Having established and tested the reduced order model, we can now use it to make investigations. The first example is to search for the worst case from the "1 minus cosine" family. The reduced model and the gust term are computed once and for all, and then the gust definition is applied in the reduced model calculation. The worst case is defined in this case as the gust producing the largest pitching response and the search was made for gust lengths between 1 and 100 semi-chords. The approach to the search was based on Kriging

interpolation, using the same procedure outlined in Ref.[22] The domain of search was divided into 100 design sites, and 30 individual gust responses were computed using the reduced model at an overall computational cost of 31 min. The worst case was computed to be for a length of 12.4 semi-chords which excites the system in its pitching frequency mode. The response is shown in Fig. 7, with the full order prediction shown to check the reduced model prediction at these conditions. The same search based on the full order model would have taken over 43 hours.

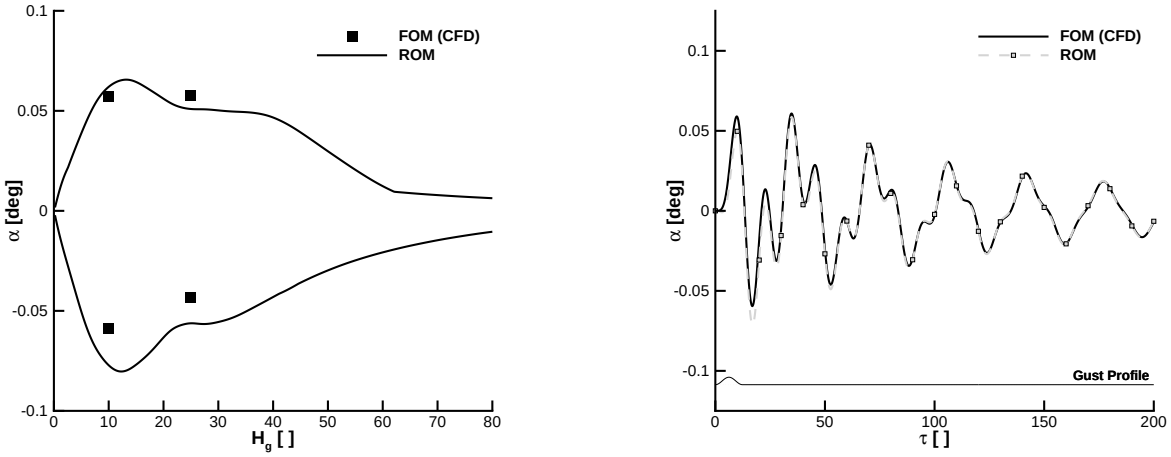

(a) Pitch, α

(b) Pitch for worst case gust, α

Figure 7. Worst case response to a "1 minus cosine" gust with intensity of 1% of the freestream speed for varying length at Mach 0.8; (b) worst case gust of length 12.4 semi-chords

IV.E. Application for Various Gusts

Continuous models of atmospheric turbulence are in the frequency domain. The Von Kármán model is a good approximation to real atmospheric spectra which tend to fall off as $f^{-5/3}$ in the frequency range of interest to aircraft response. Because the transfer function of the Von Kármán model is irrational, the rational approximation documented in Ref.[23] is used in this paper. The simulated gust input has a frequency range up to 2.5 Hz. Comparison of the full order predictions based on linear aerodynamics and CFD with the corresponding reduced models is shown in Fig. 8. For the results, the reduced models were not regenerated but those used for the discrete gust case were used here, with only the gust time history updated. The agreement between reduced models and full models is satisfactory. At Mach 0.8, the reduced model predictions in Fig. 9 are consistent with the full model response.

V. Wing Results

V.A. Test Case

The Goland wing has a chord of 6 feet and a span of 20 feet. It is a rectangular cantilevered wing with a 4% thick parabolic section. The structural model for the wing/store configuration follows the description given in Ref.[24] Four mode shapes were retained for the aeroelastic simulation. The CFD grid for Euler simulations has about 400,000 points. The mapped modes on the CFD surface grid are shown in Ref.[5] All simulations are done for a freestream Mach number of 0.85 and one degree angle of attack chosen to allow the influence of static deformation on the symmetric wing model.

V.B. Gust Interaction

The reduced model was again calculated. First the stability calculation was made using the Schur complement method. In the current work we chose to use the approximation of a Taylor expansion as described above for the aerofoil case to deal with the expensive term, $(A_{ff} - \lambda I)^{-1}$, in the formulation. Alternatively, the

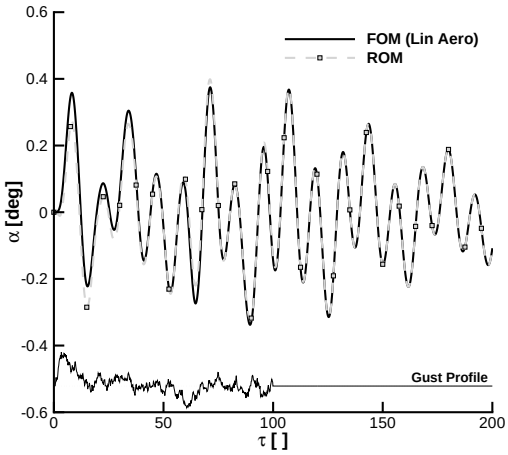

(a) Pitch, α

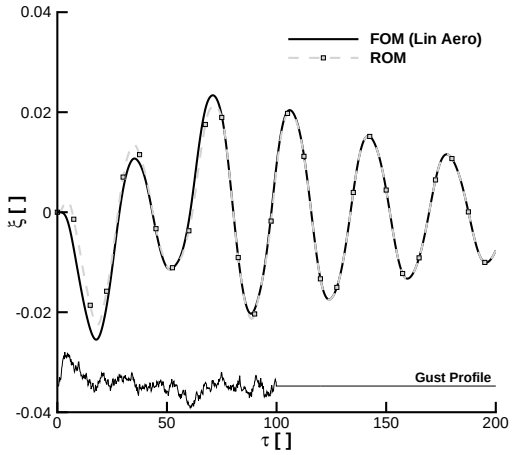

(b) Plunge, ξ

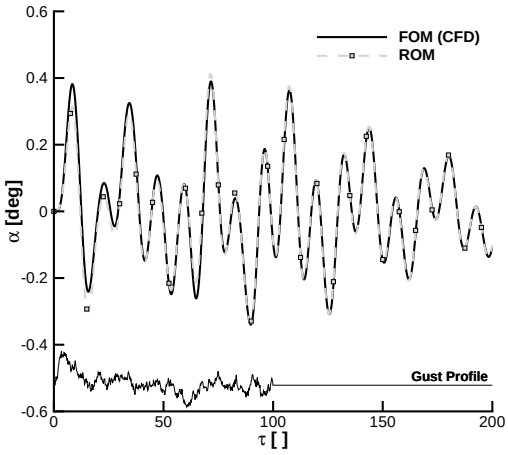

(c) Pitch, α

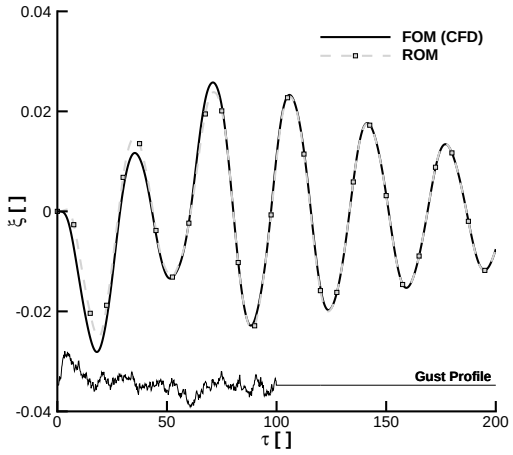

(d) Plunge, ξ

Figure 8. Response for continuous gust at Mach 0.3

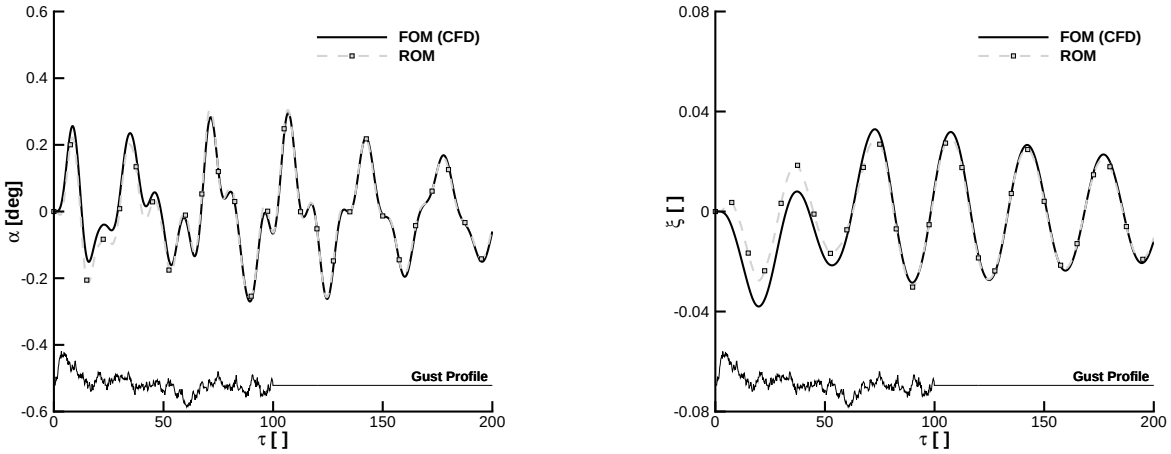

(a) Pitch, α (b) Plunge, ξ

Figure 9. Response for continuous gust at Mach 0.8

aerodynamic influence could be pre–computed for different reduced frequencies and then interpolated while solving the eigenvalue problem for decreasing values of altitude as described in Ref.[25] To solve the large sparse linear systems the method as discussed for the aerofoil problem is followed. The traces of the aeroelastic eigenvalues are shown in Fig. 10 as a function of the equivalent airspeed (EAS). The wing model shows the typical bending–torsion type of instability. The eigenvectors for the model reduction were computed at the subcritical altitude of 40,000 ft corresponding to 408 ft/s EAS.

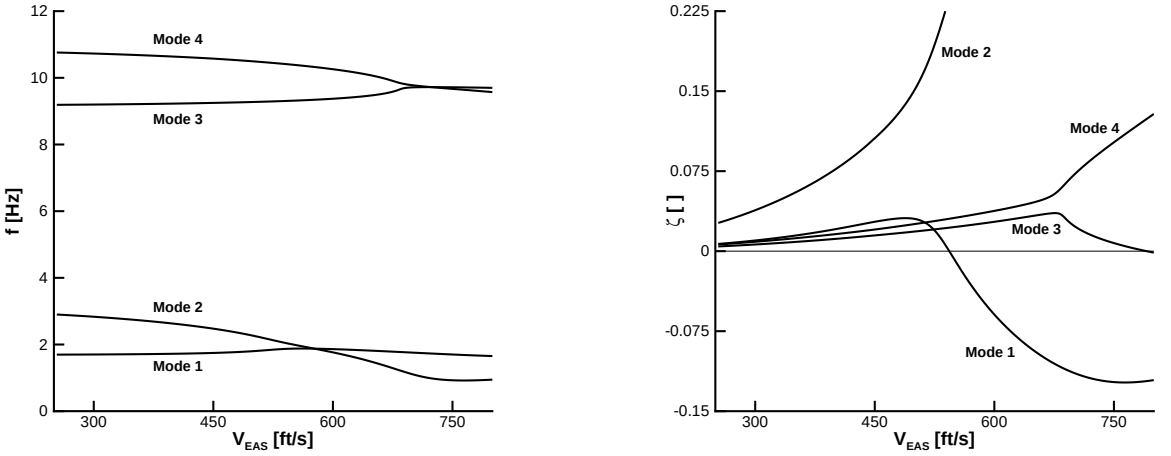

(a) Damped natural frequency, f (b) Damping ratio, ζ

Figure 10. Eigenvalue traces for Goland wing at Mach 0.85

The reduced model response to a "1 minus cosine" gust with intensity 0.1% of the freestream speed and gust length 480 ft (146.3 m) is compared with the full order result in Fig. 12 and shows good agreement. The reduced order model without the gust term is given by

$$\frac{\mathrm{d}\boldsymbol{z}}{\mathrm{d}t} = \mathrm{diag}\{\lambda_1, \lambda_2, \lambda_3, \lambda_4\}\boldsymbol{z} \tag{20}$$

where $\lambda_1 = -1.711\cdot10^{-3}+i\cdot7.904\cdot10^{-2}$, $\lambda_2 = -9.572\cdot10^{-3}+i\cdot1.193\cdot10^{-1}$, $\lambda_3 = -5.070\cdot10^{-3}+i\cdot4.229\cdot10^{-1}$, and $\lambda_4 = -8.083\cdot10^{-3}+i\cdot4.869\cdot10^{-1}$.

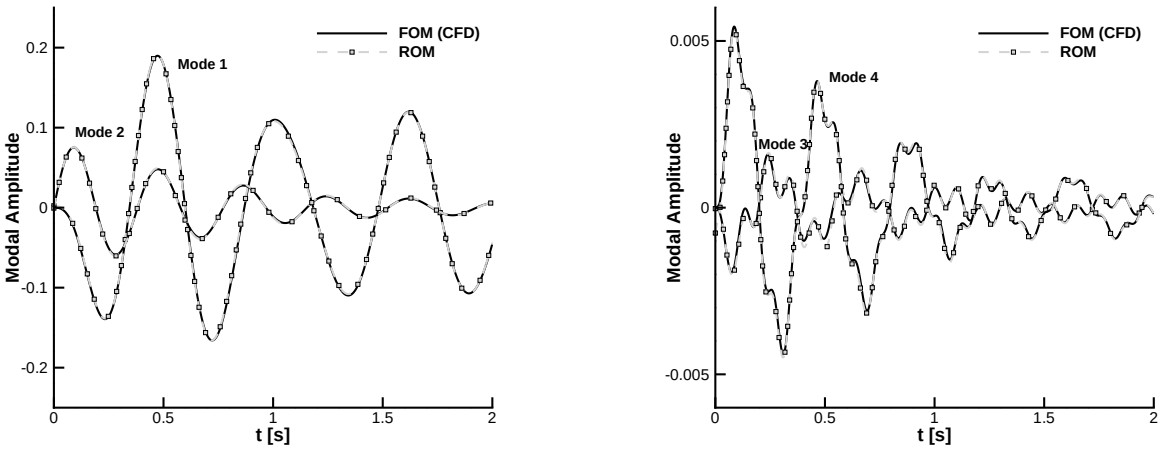

(a) Modes 1 and 2

(b) Modes 3 and 4

Figure 11. Full and reduced model responses to an initial disturbance at Mach 0.85 and 40,000 ft altitude for the Goland wing

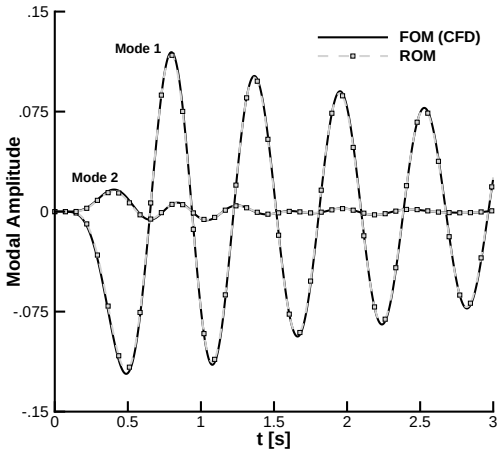

Figure 12. Full and reduced model responses to a "1 minus cosine" gust of intensity 0.001 and length 480 ft (146.3 m) at Mach 0.85 and 40,000 ft altitude for the Goland wing

The reduced model was then used to search for the worst case gust. The search was done for the "1 minus cosine" gust family with a range of gust length from 5 to 150 chord lengths. The worst case profile shown in Fig. 13 was constructed from sample calculations of the reduced model at 20 locations using Kriging interpolation. The worst case gust was found to be for 65 chords because the frequency content of the gust disturbance excites the wing in its lowest frequency mode.

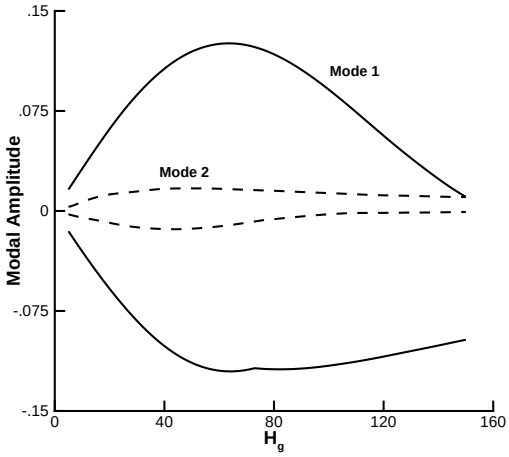

Figure 13. Worst case response to a "1 minus cosine" gust with intensity of 0.1% of the freestream speed for varying length at Mach 0.85 and 40,000 ft altitude for the Goland wing

The reduced model was then used to compute the response to a continuous gust. The gust time history is the same used for the aerofoil test case, and the responses from the reduced and full order models are shown in Fig. 14. A good agreement can be observed.

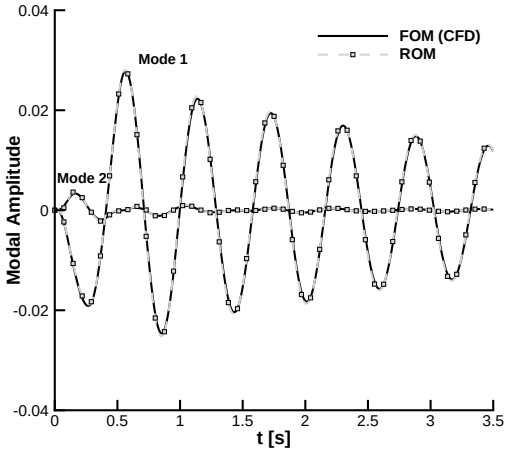

Figure 14. Response to a continuous gust for the Goland wing

VI. Conclusions

The introduction of a gust into a reduced model in a manner consistent with well established gust definitions has been considered. A new method was proposed that allows a one–off model reduction, with any gust subsequently applied to the reduced model. The formulation allows linear or nonlinear reduced models to be derived, based on a range of full order modelling options, including linear or nonlinear structural models, and linear or CFD aerodynamic models. In the current paper linear reduced models of the CFD have

proved adequate for the gust interaction simulations. Results were presented for aerofoil and wing problems to demonstrate the capability of the method. The ability of the method to enable worst case gust searches, and to allow a wide range of gusts to be computed (including continuous gusts), was demonstrated.

Future work involves the application of the method to models based on the Reynolds-averaged Navier-Stokes equations. The basic methodology is thought to generalise easily to this case. The application to full aircraft test cases is also underway, as is the use of the reduced model to design alleviation control laws.

VII. Acknowledgments

This work was supported by the U.K. Engineering and Physical Sciences Research Council (EPSRC).

References

[1]Gibson, T. E., Annaswamy, A. M., and Lavretsky, E., "Modeling for Control of Very Flexible Aircraft," AIAA Guidance, Navigation, and Control Conference, AIAA Paper 2011–6202, 2011.

[2]Dillsaver, M. J., Cesnik, C. E. S., and Kolmanovsky, I. V., "Gust Load Alleviation Control for Very Flexible Aircraft," AIAA Atmospheric Flight Mechanics Conference, AIAA Paper 2011–6368, 2011.

[3]Raveh, D. E., "Gust-Response Analysis of Free Elastic Aircraft in the Transonic Flight Regime," Journal of Aircraft, Vol. 48, No. 4, 2011, pp. 1204–1211, doi: 10.2514/1.C031224.

[4]Parameswaran, V. and Baeder, J. D., "Indicial Aerodynamics in Compressible Flow - Direct Computational Fluid Dynamic Calculations," Journal of Aircraft, Vol. 34, No. 1, 1997, pp. 131–133.

[5]Badcock, K. J., Timme, S., Marques, S., Khodaparast, H., Prandina, M., Mottershead, J. E., Swift, A., Da Ronch, A., and Woodgate, M. A., "Transonic Aeroelastic Simulation for Instability Searches and Uncertainty Analysis," Progress in Aerospace Sciences, Vol. 47, No. 5, 2011, pp. 392–423, doi: 10.1016/j.paerosci.2011.05.002.

[6]Woodgate, M. A. and Badcock, K. J., "Fast Prediction of Transonic Aeroelastic Stability and Limit Cycles," AIAA Journal, Vol. 45, No. 6, 2007, pp. 1370–1381, doi: 10.2514/1.25604.

[7]Badcock, K. J., Woodgate, M. A., Allan, M. R., and Beran, P. S., "Wing-Rock Limit Cycle Oscillation Prediction based on Computational Fluid Dynamics," Journal of Aircraft, Vol. 45, No. 3, 2008, pp. 954–961, doi: 10.2514/1.32812.

[8]Da Ronch, A., Badcock, K. J., Wang, Y., Wynn, A., and Palacios, R. N., "Nonlinear Model Reduction for Flexible Aircraft Control Design," AIAA Atmospheric Flight Mechanics Conference, AIAA Paper 2012–4404, 2012.

[9]Kennett, D. J., Timme, S., Angulo, J., and Badcock, K. J., "An Implicit Meshless Method for Application in Computational Fluid Dynamics," International Journal for Numerical Methods in Fluids, Vol. 71, No. 8, 2013, pp. 1007–1028, doi: 10.1002/fld.3698.

[10]Kennett, D. J., Timme, S., Angulo, J., and Badcock, K. J., "Semi-Meshless Stencil Selection for Anisotropic Point Distributions," International Journal of Computational Fluid Dynamics, Vol. 26, No. 9–10, 2012, pp. 463–487, doi: 10.1080/10618562.2012.744450.

[11]Badcock, K. J., Richards, B. E., and Woodgate, M. A., "Elements of computational fluid dynamics on block structured grids using implicit solvers," Progress in Aerospace Sciences, Vol. 36, No. 5–6, 2000, pp. 351–392, doi: 10.1016/S0376-0421(00)00005-1.

[12]Lee, B. H. K., Gong, L., and Wong, Y. S., "Analysis and Computation of Nonlinear Dynamic Response of a Two-Degree-of-Freedom System and Its Application in Aeroelasticity," Journal of Fluids and Structures, Vol. 11, No. 3, 1997, pp. 225–246, doi: 10.1006/jfls.1996.0075.

[13]Meirovitch, L., Dynamics and Control of Structures, Wiley, New York, 1989, pp. 93–98.

[14]Pettit, C. L. and Beran, P. S., "Effects of parametric uncertainty on airfoil limit cycle oscillation," Journal of Aircraft, Vol. 40, No. 5, 2003, pp. 1004–1006.

[15]Badcock, K. J., Khodaparast, H. H., Timme, S., and Mottershead, J. E., "Calculating the Influence of Structural Uncertainty on Aeroelastic Limit Cycle Response," 52nd AIAA/ASME/ASCE/AHS/ASC Structures, Structural Dynamics, and Materials Conference, AIAA-2011-1741, 2011.

[16]Badcock, K. J. and Woodgate, M. A., "Bifurcation Prediction of Large-Order Aeroelastic Models," AIAA Journal, Vol. 48, No. 6, 2010, pp. 1037–1046, doi: 10.2514/1.40961.

[17]Hoblit, F. M., Gust Loads on Aircraft: Concepts and Applications, American Institute of Aeronautics and Astronautics, Reston, VA, USA, 1988.

[18]Da Ronch, A., On the Calculation of Dynamic Derivatives Using Computational Fluid Dynamics, Ph.D. thesis, University of Liverpool, Liverpool, U.K., March 2012.

[19]Badcock, K. J., Woodgate, M., and Richards, B. E., "Hopf Bifurcation Calculations for a Symmetric Airfoil in Transonic Flow," AIAA Journal, Vol. 42, No. 5, 2004, pp. 883–892, doi: 10.2514/1.9584.

[20]"Inviscid Flowfield Methods," Tech. Rep. Fluid Dynamics Panel Working Group, AGARD AR 211, 1985.

[21]McCracken, A., Da Ronch, A., Timme, S., and Badcock, K. J., "Solution of linear systems in Fourier-based methods for aircraft applications," International Journal of Computational Fluid Dynamics, 2013.

[22]Da Ronch, A., Ghoreyshi, M., and Badcock, K. J., "On the Generation of Flight Dynamics Aerodynamic Tables by Computational Fluid Dynamics," Progress in Aerospace Sciences, Vol. 47, No. 8, 2011, pp. 597–620, doi: 10.1016/j.paerosci.2011.09.001.

[23]Campbell, C. W., "Monte Carlo Turbulence Simulation Using Rational Approximations to Von Kármán Spectra," AIAA Journal, Vol. 24, No. 1, 1986, pp. 62–66, doi: 10.2514/3.9223.

[24]Beran, P. S., Khot, N. S., Eastep, F. E., Snyder, R. D., and Zweber, J. V., "Numerical analysis of store–induced limit–cycle oscillation," Journal of Aircraft, Vol. 41, No. 6, 2004, pp. 1315–1326.

[25]Timme, S., Marques, S., and Badcock, K. J., "Transonic aeroelastic stability analysis using a kriging–based Schur complement formulation," AIAA Journal, Vol. 49, No. 6, 2011, pp. 1202–1213.